Controlling gas selectivity in molecular porous liquids by tuning the cage window size

Benjamin D. Egleston,[a] Konstantin V. Luzyanin,[b] Michael C. Brand,[a] Rob Clowes,[a] Michael E. Briggs,[a] Rebecca L. Greenaway*[b] and Andrew I. Cooper*[a]

[a]Department of Chemistry and Materials Innovation Factory, University of Liverpool, Oxford Street, Liverpool, L7 3NY, UK; [b]Department of Chemistry, University of Liverpool, Crown Street, Liverpool, L69 7ZD, UK.

E-mail: rebecca.greenaway@liverpool.ac.uk, aicooper@liverpool.ac.uk

Abstract

Control of pore window size is the standard approach for tuning gas selectivity in porous solids. Here, we present the first example where this is translated into a molecular porous liquid formed from organic cage molecules. Reduction of the cage window size by chemical synthesis switches the selectivity from Xe-selective to CH_4-selective, which is understood using ^{129}Xe, ^{1}H, and pulsed-field gradient NMR spectroscopy.

Table of Contents

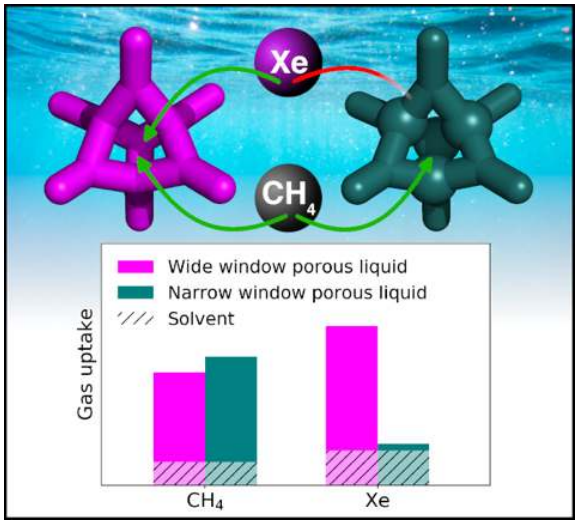

Porous liquids (PLs) are a new class of porous material.[1–3] They differ from conventional liquids because they have permanent, intrinsic micropores, in contrast to the transient, sub-molecular extrinsic voids found in all liquids (Figure 1). PLs can be categorized by their composition: Type 1 PLs are neat molecular liquids containing internal cavities; Type 2 PLs (Figure 1b) are solutions of porous molecules in a solvent that is size-excluded from the pores; and Type 3 PLs are dispersions of porous particles suspended in a cavity excluded liquid.[4] Examples of all three types of PL have been described recently,[5–12] and molecular simulations have led to a better understanding of their microstructure.[13–16]

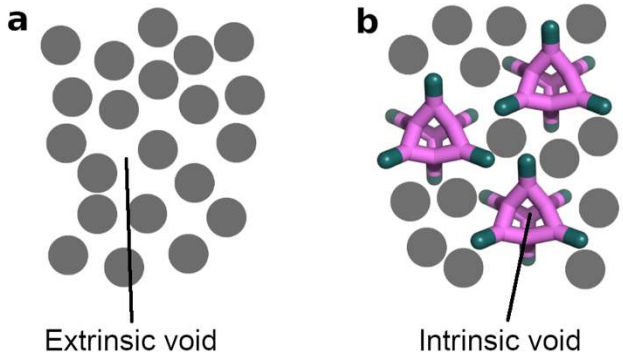

Figure 1. Diagram representing (a) conventional molecular liquids and (b) Type 2 molecular porous liquids. Solvent molecules are displayed as grey circles.

Porous organic cages (POCs) are a relatively new class of microporous solids that, unlike extended frameworks, are constructed from discrete organic molecules.[17–19] POCs are shape-persistent molecules containing an internal cavity, which allows them to be dissolved in solvents while retaining their pore structure, setting them apart from many other types of insoluble porous materials, such as zeolites, metal organic frameworks and covalent organic frameworks.[20] The discrete nature of POCs has led to attempts to produce Type 1 PLs,[13,21] and to the successful production of Type 2 PLs.[1,22] The latter PLs were obtained by dissolving POCs at high concentration in a solvent that was too bulky to pass through the windows of the cage. Recently, we investigated the uptake, gas selectivity and diffusion of different gases in a PL consisting of a scrambled [4+6] imine POC mixture dissolved in a bulky chlorinated solvent, hexachloropropene (HCP).[22] Dynamic covalent scrambling was used to produce highly soluble vertex-disordered POC mixtures.[23] The POC used in our first scrambled cage PL, **CC3^3:13^3**-*R* (Scheme 1), was based on the scrambling of the discrete POCs **CC3** and **CC13**. The gas uptake capacity of this PL correlated with the heats of adsorption of the respective solid, crystalline POC, **CC3**. This showed that the thermodynamic gas selectivity of the PL was governed by the structure and interactions of the constituent POC, suggesting to us a scheme for tuning selectivity in PLs.

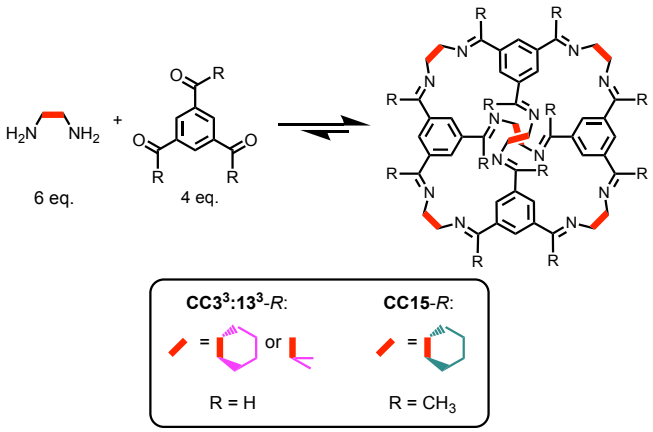

Scheme 1. Synthesis of POCs for PLs. Conditions: (**CC3³:13³**-*R*) dichloromethane, room temperature, 72 h; (**CC15**-*R*) dichloromethane, 3Å molecular sieves, 50 °C, reverse Dean Stark, 24 h.

Here, we exploited the synthetic modularity of POC molecules to produce PLs with different gas selectivities. This is the first example of tuning gas selectivity in a Type 2 PL by using chemistry. The imine POC, **CC15**-*R* (Scheme 1), is a close analogue of **CC3**-*R* that has smaller pore windows (1.7 Å vs 4.0 Å respectively), which are partially occluded by methyl groups (Figure 2a).[24] The inclusion of methyl groups in the windows also leads to a reduction in cavity size (OPT pore sizes calculated using pywindow[25]: **CC3³:13³**-*R* 5.85 Å, **CC15**-*R* 4.61 Å). As a result, **CC15**-*R* adsorbs very little N_2 in the solid state, quite unlike **CC3**-*R* (Figure 2b). **CC15**-*R* still adsorbs smaller gas molecules, such as H_2; this is because the window size, and the smaller cavity size, modulates the gas selectivity in the solid, crystalline state.

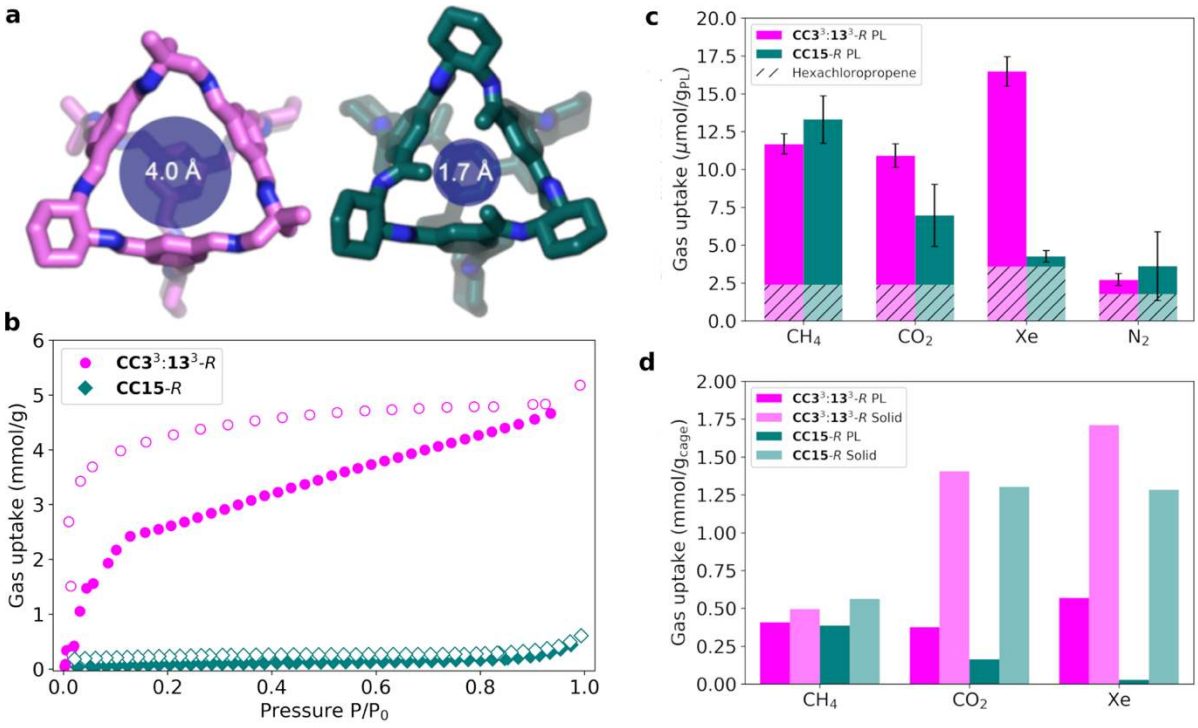

Figure 2. (a) Structures of the *trans*-**3³13³** component of the scrambled cage mixture **CC3³:13³**-*R* (magenta, left) and **CC15**-*R* (teal, right) with the average window diameters calculated using the pywindow package;[25] (b) N_2 adsorption (filled) and desorption (empty) isotherms for **CC3³:13³**-*R* and **CC15**-*R*; (c) Uptake by volumetric gas

evolution for CH_4, CO_2, Xe, and N_2 for **CC3^3:13^3**-*R* (magenta) and **CC15**-*R* (teal) PLs, compared with uptake in hexachloropropene (HCP, dashed lines, overlaid). **CC3^3:13^3**-*R* PL at 4% w/v and **CC15**-*R* PL at 5% w/v; (d) Comparison of gas uptake in the liquid and solid state for each POC. Uptake for PLs is adjusted by subtracting the native gas capacity of HCP to show the POC uptake only, and normalized to the mass of cage present.

Here we sought to translate this principle for the first time into PLs. **CC15**-*R* was found to be soluble in HCP at a concentration (50 mg_{cage} in 1 mL_{HCP}, 5% w/v) that was high enough to investigate gas uptake properties, albeit at a significantly lower concentration than our previous **CC3^3:13^3**-*R* scrambled cage in this solvent (200 mg_{cage} in mL_{HCP}, 20% w/v).[22] Even though the solubility of **CC15**-*R* appears low when benchmarked against a scrambled cage mixture, it should be noted that this solubility is still much higher than for the structurally related **CC3**-*R* in HCP (<15.6 mg_{cage} in 1 mL_{HCP}). We also tried to increase the solubility by forming a scrambled analogue of **CC15**-*R*, but HPLC analysis indicated that only **CC15**-*R* was formed; no scrambling occurred, possibly because the three methyl groups in 1,3,5-triacetylbenzene clash sterically with the methyl groups in 1,2-diamino-2-methylpropane, preventing scrambling.

To compare these PL systems directly, equimolar solutions (39 μmol_{cage} in 1 mL_{HCP}) were prepared in HCP of **CC3^3:13^3**-*R* (40 mg_{cage} in 1 mL_{HCP}, 4% w/v) and **CC15**-*R* (5% w/v), thus ensuring the same volumetric density of pore cavities in each case. Gas uptakes were determined for both PLs for CH_4, CO_2, Xe, and N_2, using a guest displacement method that we described previously.[22] With the exception of Xe in **CC15**-*R* PL, the gas uptake was enhanced in the PLs in all cases compared to the neat solvent (Figure 2c). Because of the significantly lower cage concentration in these two PLs, gas uptakes were reduced for all gases with respect to our previous 20% w/v scrambled PL; for example, the CH_4 uptake in the **CC3^3:13^3**-*R* scrambled PL was 45.8 $\mu mol/g_{PL}$ at 20% w/v[22] compared to 11.7 $\mu mol/g_{PL}$ at 4% w/v here. In the case of N_2, the improvement in uptake with respect to the neat solvent was low for both PLs compared to neat HCP (Figure 2c), reflecting our previous observations at higher cage concentrations.[22] For other gases, despite the lower pore concentration, the gas solubility improvements were more marked with up to a ~5.5 fold increase over the neat solvent, and there were large differences between the two PLs. The Xe uptake in **CC3^3:13^3**-*R* PL (16.6 $\mu mol/g_{PL}$) was almost four times that measured for **CC15**-*R* PL (4.3 $\mu mol/g_{PL}$) at the same pore concentration. The reduction in Xe uptake can be attributed to the methyl groups in **CC15**-*R*, which encroach on the cage windows and available pore volume that is accessible to Xe in **CC3^3:13^3**-*R*. The **CC3^3:13^3**-*R* PL absorbs more Xe than the other gases tested, reflecting the thermodynamic preference for Xe observed previously in these imine POCs,[26] but this is totally lost in the PL derived from the methylated analogue, **CC15**-*R*. We carried out a much longer gas saturation experiment (Table S2) to rule out this being a kinetic limitation due to the saturation time, and found no increase in uptake. Furthermore, the **CC15**-*R* PL absorbs CH_4 most preferentially, and more effectively than **CC3^3:13^3**-*R*; that is, the **CC3^3:13^3**-*R* PL shows preferential uptake for Xe, while the **CC15**-*R* PL is CH_4 shows preferential uptake for CH_4.

The gas uptake in these two PLs can be compared directly to the gas uptake in the corresponding POC solids by subtracting the baseline solubility in HCP and normalizing to the mass of cage present (Figure 2d). Nitrogen was not included in these comparisons since the solid-state sorption measurements were carried out at 77 K, not at 298 K. Direct comparison of the gas uptakes in the two solid POCs shows similar trends (**CC3^3:13^3**-*R* Xe>CO_2>CH_4, **CC15**-*R* CO_2≈Xe>CH_4). The gas uptake in **CC3^3:13^3**-*R* directly mirrors the isosteric heats of adsorption that were calculated previously for **CC3**-*R* (Xe 31.31

kJ.mol^{-1}, CO_2 27.73 kJ.mol^{-1}, CH_4 22.05 kJ.mol^{-1}).[22] **CC15**-*R*, however, shows a weaker correlation: the CO_2 and Xe uptakes are similar, and both are reduced compared to **CC3^3:13^3**-*R*. Previously, for **CC3**-*R*, it was found that CO_2 has a preference to occupy the space in the crystal structure that corresponds to the cage portals, as well as having favorable electrostatic interactions with the imine bonds in the POC.[27] Therefore, the CO_2 uptake in **CC15**-*R* is reduced compared to **CC3^3:13^3**-*R* since the addition of the window-occluding methyl groups inhibits both of these effects. Xe has a high affinity for the pore cavity in **CC3**-*R* due to its excellent fit.[26] The methyl groups in **CC15**-*R* reduce the ability for Xe to occupy this cavity, resulting in a lower gas uptake in the solid. However, the porosity is not completely lost for these gases in the solid state because the methyl groups in **CC15**-*R* only affect the intrinsic pores, leaving the extrinsic pores intact.

When comparing between the solid and liquid state for CH_4, the mass-normalized gas uptake in the cages in the PLs (0.409 mmol/g_{cage} for **CC3^3:13^3**-*R* PL, 0.386 mmol/g_{cage} for **CC15**-*R* PL) is broadly comparable to the uptake observed in the solid state (0.495 mmol/g_{cage} for **CC3^3:13^3**-*R* solid, 0.562 mmol/g_{cage} **CC15**-*R* solid). This suggests that, like Xe and CO_2, CH_4 does not have a preference for the extrinsic cavities in the solid state. However the kinetic diameter (3.8 Å)[28] is smaller than the cavities in the cages (**CC3^3:13^3**-*R* 5.85 Å, **CC15**-*R* 4.61 Å), and hence CH_4 is able to occupy the cage cavities both in the solid and liquid state. However, this does not hold for Xe and CO_2. The solid state CO_2 uptakes for the cages (1.407 mmol/g_{cage} for **CC3^3:13^3**-*R* solid, 1.304 mmol/g_{cage} for **CC15**-*R* solid) are around one order of magnitude higher than the mass-normalized uptakes for the PLs (0.375 mmol/g_{cage} for **CC3^3:13^3**-*R* PL, 0.164 mmol/g_{cage} for **CC15**-*R* PL). This difference can be attributed, at least in part, to the interconnected solid-state porosity that comprises both intrinsic pores (inside cages) and extrinsic pores (between cages), whereas these PLs only have intrinsic pores. Furthermore, while CO_2 has a tendency to occupy the portal sites in solid POCs, the cages in these PLs are solvated, meaning that these portal sites do not exist. Hence, uptake enhancement is due solely to the intrinsic pore.[29] This also explains the reduction in CO_2 capacity in the **CC15**-*R* PL compared to the **CC3^3:13^3**-*R* PL, as the methyl groups further inhibit occupancy of CO_2 in the portal site, as well as limiting the electrostatic interaction.

For Xe, there is a much larger disparity in gas uptakes in these PLs (0.568 mmol/g_{cage} for **CC3^3:13^3**-*R* PL, 0.027 mmol/g_{cage} for **CC15**-*R* PL); this does not reflect the solid state trend for these POCs, where both of the cage materials adsorb significant amounts of Xe (1.710 mmol/g_{cage} for **CC3^3:13^3**-*R* solid, 1.283 mmol/g_{cage} for **CC15**-*R* solid). While the uptake of Xe is reduced in the **CC3^3:13^3**-*R* PL compared to the solid state, it still mirrors the calculated isosteric heats for **CC3**-*R* due to its near-ideal cavity size. In the **CC15**-*R* PL,[26] the methyl groups reduce the ability for Xe to occupy this cavity. Effectively, the Xe uptake has been 'shut off' in **CC15**-*R* compared to **CC3^3:13^3**-*R* when translated into the PL state due to the window occlusion and reduced pore size. This suggests that the Xe uptake in solid **CC15**-*R* may be due mostly to extrinsic intermolecular pores.[24]

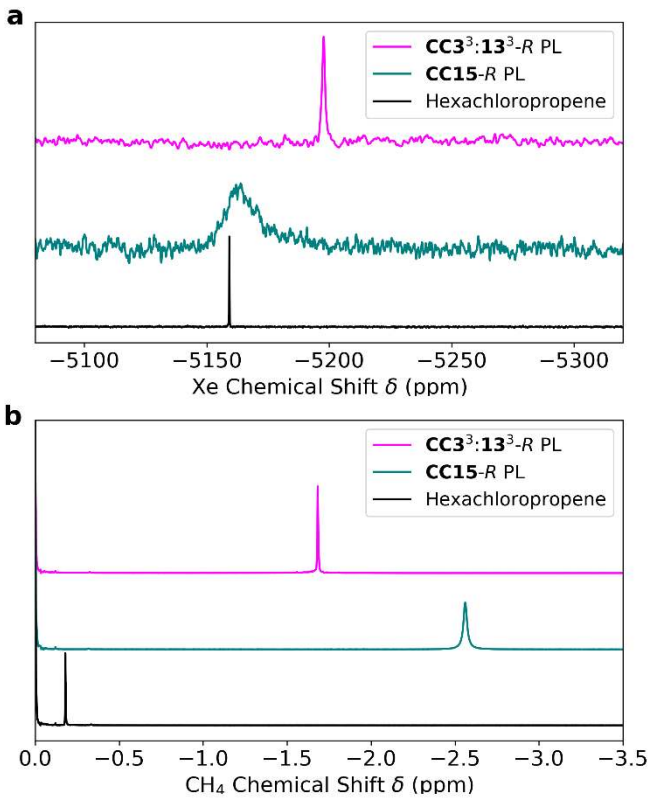

Figure 3. (a) ^{129}Xe and (b) ^{1}H NMR spectra for Xe and CH_4 gas in **CC3^3:13^3**-*R* and **CC15**-*R* PLs compared to in neat HCP. **CC3^3:13^3**-*R* PL at 4% w/v and **CC15**-*R* PL at 5% w/v.

To investigate these differences, ^{1}H and ^{129}Xe NMR spectroscopy were used to characterize the chemical environment of the gases in both the PLs and in the neat solvent, HCP (Figure 3). This allowed us to probe the extent of gas binding in each PL, since the ^{1}H and ^{129}Xe nuclei are highly sensitive to their chemical environment, leading to upfield shifts when the cage cavities are occupied. In the ^{129}Xe spectra, the **CC3^3:13^3**-*R* PL exhibits a large upfield shift relative to HCP ($\Delta\delta$ = −38.6 ppm), whereas this shift is relatively small for the **CC15**-*R* PL ($\Delta\delta$ = −4.7 ppm), where the Xe signal is also weak. This shows that the Xe gas cannot easily occupy the pores in the **CC15**-*R* PL, whereas in **CC3^3:13^3**-*R* PL, the much larger downfield shift is due to the Xe gas readily occupying the cage cavities. This confirms that Xe uptake in the **CC15**-*R* PL is switched off by reducing the cage window size.

This relationship between gas uptake and downfield chemical shift also holds for CH_4. In both PLs, there is a significant upfield shift compared to HCP ($\Delta\delta$ = −1.50 ppm in **CC3^3:13^3**-*R* PL, $\Delta\delta$ = −2.38 ppm in **CC15**-*R* PL). The larger shift observed in the **CC15**-*R* PL shows that CH_4 is experiencing a larger shielding effect. ^{1}H NMR spectroscopy can be used to quantify the saturation concentrations of CH_4 by using a sealed, calibrated d_2-DCM/TMS capillary. The gas uptakes measured by NMR (17.5 µmol/g_{PL} in **CC3^3:13^3**-*R* PL, 21.5 µmol/g_{PL} in **CC15**-*R* PL) are higher than for the gas displacement measurements (11.6 µmol/g_{PL} in **CC3^3:13^3**-*R* PL, 13.3 µmol/g_{PL} in **CC15**-*R* PL), reflecting trends in a previous study.[22] This is because gas evolution experiments cannot release all of the gas dissolved in a PL because of the baseline gas solubility in both HCP and in the displacement solvent.

Next, pulsed-field gradient (PFG) NMR experiments were carried out to measure diffusion of CH_4 in the two PL systems. The results of these experiments are related to the binding of CH_4 in the PLs. The

measured diffusion co-efficients for each POC (6.14×10^{-11} m^2/s for **CC3^3:13^3**-*R*, 6.33×10^{-11} m^2/s for **CC15**-*R*) and sample viscosities (Table S6) were used to calculate solvodynamic radii using the Stokes-Einstein equation for the two POCs in the PLs (8.2 Å for **CC3^3:13^3**-*R*, 8.3 Å for **CC15**-*R*); these values agree with the expected size of a [4+6] imine cage.[30] The diffusion co-efficients for CH_4 in the two PLs (5.43×10^{-10} m^2/s in **CC3^3:13^3**-*R* PL, 4.58×10^{-10} m^2/s in **CC15**-*R* PL) are significantly lower than in neat HCP (1.34×10^{-9} m^2/s), indicating that association of the gas with the cage is occurring and that this is observable by PFG NMR. Since the CH_4 has not adopted the same diffusion co-efficient as the POCs, this indicates that the gas is in dynamic equilibrium on the NMR timescale between the POC cavity and the HCP solvent. Therefore, this information can be used to calculate the fraction of gas molecules occupying the cage cavities (X_{occ}), as well as the association constant (K_a) for each system.[31] In the **CC3^3:13^3**-*R* PL, $X_{occ} = 0.49$, while for the **CC15**-*R* PL $X_{occ} = 0.60$. The corresponding association constants for CH_4 in each PL can be calculated from the diffusion co-efficients measured for CH_4 in each PL ($K_a = 2.71 \times 10^4$ mol^{-1} dm^3 for CH_4 in **CC3^3:13^3**-*R* PL, $K_a = 4.36 \times 10^4$ mol^{-1} dm^3 for CH_4 in **CC15**-*R* PL). These measurements confirm that CH_4 more preferentially occupies the cavity in the **CC15**-*R* PL than in the **CC3^3:13^3**-*R* PL, in keeping with the gas uptake measurements, where the **CC15**-*R* PL absorbs more CH_4 (Figure 2c).

Retention of CH_4 in these PLs was also examined by measuring the kinetics of gas loss using ^{1}H NMR spectroscopy. The CH_4 concentration at a series of time intervals was recorded and the rate of loss of CH_4 while open to air was compared after normalizing the curves to the saturation concentration for each porous liquid (Figure S13). After 1 day, the **CC15**-*R* PL retained 23% more of the initial CH_4 concentration when compared with **CC3^3:13^3**-*R* PL, and over a period of *ca.* 2 days, the CH_4 was lost more slowly from the **CC15**-R PL than from the **CC3^3:13^3**-*R* PL. This shows that narrowing the pore diameter in the molecular cage component in a PL can also improve the retention of gases over time.

In summary, modification of the window and pore size in POCs can modulate the gas selectivity in PLs, demonstrating that a key structure-function design principle in porous solids can be translated into these new materials: for example, we can shut off Xe absorption by narrowing the cage window, which also reduces the pore size, in the **CC15**-*R* PL (Figure 2d). There are also some differences between these two types of porous materials: for example, for CO_2 (Figure 2d), the amount of gas per cage is significantly lower in the PLs, probably because the PLs, unlike the corresponding porous solids, lack intermolecular pores between cages that allow multilayer adsorption and pore filling as saturation is approached.

In the longer term, this offers the potential of flowable, gas-selective liquids for separation processes; for example, where a gas-selective PL is cycled between a cold absorption zone and a hot desorption zone. The relatively modest viscosities of these PLs (up to 11.7 cP at 20% w/v)[22] should allow such processes. The selectivity might be increased further by designing analogous cage materials with higher solubilities; likewise, eliminating the solvent altogether could enhance selectivity since the carrier solvent in these Type 2 PLs is relatively unselective, although in that case, liquid viscosity might be a major challenge.

Acknowledgements

We thank the Engineering and Physical Sciences Research Council (EPSRC) under the Grants EP/N004884/1 and EP/R005710/1, and the European Research Council under FP7, RobOT, ERC Grant

Agreement No. 321156, for financial support. R.L.G. thanks the Royal Society for a University Research Fellowship. We acknowledge the MicroBioRefinery for assistance with QTOF-MS measurements. We thank Dr. Tom Hasell (University of Liverpool) and Prof. Stuart James (Queen's University Belfast) for helpful discussions.

Conflict of Interest

There are no conflicts to declare.

References

[1] N. Giri, M. G. Del Pópolo, G. Melaugh, R. L. Greenaway, K. Rätzke, T. Koschine, L. Pison, M. F. C. Gomes, A. I. Cooper, S. L. James, *Nature* **2015**, *527*, 216–220.

[2] S. L. James, *Adv. Mater.* **2016**, *28*, 5712–5716.

[3] A. I. Cooper, *ACS Cent. Sci.* **2017**, *3*, 544–553.

[4] N. O'Reilly, N. Giri, S. L. James, *Chem. - A Eur. J.* **2007**, *13*, 3020–3025.

[5] J. Zhang, S. H. Chai, Z. A. Qiao, S. M. Mahurin, J. Chen, Y. Fang, S. Wan, K. Nelson, P. Zhang, S. Dai, *Angew. Chemie - Int. Ed.* **2015**, *54*, 932–936.

[6] P. Li, J. A. Schott, J. Zhang, S. M. Mahurin, Y. Sheng, X. Hu, G. Cui, D. Yao, S. Brown, Y. Zheng, et al., *Angew. Chemie Int. Ed.* **2017**, *56*, 14958.

[7] S. Liu, J. Liu, X. Hou, T. Xu, J. Tong, J. Zhang, B. Ye, B. Liu, *Langmuir* **2018**, *34*, 3654–3660.

[8] X. Li, Y. Ding, L. Guo, Q. Liao, X. Zhu, *Energy* **2019**, *171*, 109–119.

[9] P. Li, H. Chen, J. A. Schott, B. Li, Y. Zheng, **2019**, 1515–1519.

[10] W. Shan, P. F. Fulvio, L. Kong, J. A. Schott, C. L. Do-Thanh, T. Tian, X. Hu, S. M. Mahurin, H. Xing, S. Dai, *ACS Appl. Mater. Interfaces* **2018**, *10*, 32–36.

[11] T. Shi, Y. Zheng, T. Wang, P. Li, Y. Wang, D. Yao, *ChemPhysChem* **2018**, *19*, 130–137.

[12] X. Wang, D. Shang, S. Zeng, Y. Wang, X. Zhang, X. Zhang, J. Liu, *J. Chem. Thermodyn.* **2019**, *128*, 415–423.

[13] G. Melaugh, N. Giri, C. E. Davidson, S. L. James, M. G. Del Pópolo, *Phys. Chem. Chem. Phys.* **2014**, *16*, 9422–31.

[14] F. Zhang, F. Yang, J. Huang, B. G. Sumpter, R. Qiao, *J. Phys. Chem. B* **2016**, *120*, 7195–7200.

[15] F. Zhang, Y. He, J. Huang, B. G. Sumpter, R. Qiao, *J. Phys. Chem. C* **2017**, *121*, 12426.

[16] M. Costa Gomes, L. Pison, C. Červinka, A. Padua, *Angew. Chemie Int. Ed.* **2018**, *54*, 932-936.

[17] F. Beuerle, B. Gole, *Angew. Chemie - Int. Ed.* **2018**, 2–31.

[18] P. S. Mukherjee, K. Acharyya, *Angew. Chemie Int. Ed.* **2019**, DOI 10.1002/anie.201900163.

[19] M. Mastalerz, *Acc. Chem. Res.* **2018**, *51*, 2411–2422.

[20] T. Hasell, A. I. Cooper, *Nat. Rev. Mater.* **2016**, *1*, 16053.

[21] N. Giri, C. E. Davidson, G. Melaugh, M. G. Del Pópolo, J. T. a. Jones, T. Hasell, A. I. Cooper, P. N. Horton, M. B. Hursthouse, S. L. James, *Chem. Sci.* **2012**, *3*, 2153.

[22] R. L. Greenaway, D. Holden, E. G. B. Eden, A. Stephenson, C. W. Yong, M. J. Bennison, T. Hasell, M. E. Briggs, S. L. James, A. I. Cooper, *Chem. Sci.* **2017**, *8*, 2640–2651.

[23] S. Jiang, J. T. a Jones, T. Hasell, C. E. Blythe, D. J. Adams, A. Trewin, A. I. Cooper, *Nat. Commun.* **2011**, *2*, 207.

[24] A. G. Slater, P. S. Reiss, A. Pulido, M. A. Little, D. L. Holden, L. Chen, S. Y. Chong, B. M. Alston, R. Clowes, M. Haranczyk, et al., *ACS Cent. Sci.* **2017**, *3*, 734–742.

[25] M. Miklitz, K. E. Jelfs, *J. Chem. Inf. Model.* **2018**, *58*, 2387–2391.

[26] L. Chen, P. S. Reiss, S. Y. Chong, D. Holden, K. E. Jelfs, T. Hasell, M. A. Little, A. Kewley, M. E. Briggs, A. Stephenson, et al., *Nat Mater* **2014**, *13*, 954–960.

[27] T. Hasell, J. A. Armstrong, K. E. Jelfs, F. H. Tay, K. M. Thomas, S. G. Kazarian, A. I. Cooper, *Chem. Commun.*, **2013**, *49*, 9410-9412.

[28] Robeson L. M., *J. Membrane. Sci.*, **1991**, *62*, 165-185.

[29] S. Jiang, K. E. Jelfs, D. Holden, T. Hasell, S. Y. Chong, M. Haranczyk, A. Trewin, A. I. Cooper, *J. Am.Chem. Soc.*, **2013**, *135*, 17818-17830.

[30] R. L. Greenaway, V. Santolini, M. J. Bennison, B. M. Alston, C. J. Pugh, M. A. Little, M. Miklitz, E. G. B. Eden-Rump, R. Clowes, A. Shakil, et al., *Nat. Commun.* **2018**, *9*, 2849.

[31] K. S. Cameron, L. Fielding, *J. Org. Chem.* **2001**, *66*, 6891–6895.